J Ther Eng, Vol. 9, No. 6, pp. 1428−1441, November, 2023

Journal of Thermal Engineering
Web page info: https://jten.yildiz.edu.tr
DOI: 10.18186/thermal.00000

Journal of Thermal Engineering

Research Article

Numerical simulation to study mixing vane spacer effects on heat transfer performance of supercritical pressure fluid in an annular channel

Satish Kumar DHURANDHAR[1,*], Shobha Lata SINHA[1], Shashi Kant VERMA[2]

[1]*Department of Mechanical Engineering, National Institute of Technology Raipur, (C.G), 492010, India*
[2]*Department of Mechanical Engineering, National Institute of Technology Durgapur, West Bengal, 713209, India*

ARTICLE INFO

Article history
Received: 02 July 2021
Revised: 29 October 2021
Accepted: 04 November 2021

Keywords:
Supercritical Pressure; Mixing Vane Spacer; Heat Transfer; CFD; Vertical Annular Flow

ABSTRACT

The spacer represents an essential part in the nuclear fuel rod. Spacer grid with mixing vanes in fuel rod bundle of nuclear reactor core has a significant impact on heat transfer performance in downstream to grid spacer. Grid Spacers are located on the nuclear fuel rod assembly to hold suitable clearance among the rods in a bundle. The objective of this paper is to study the enhanced heat transfer performance of R134a at supercritical pressure 4.5 MPa near downstream to mixing vane spacer in a vertical channel of annular flow. A spacer of 0.38 blockage ratio with mixing vanes, situated at mid-span of an annular channel is used in the present work. Numerical simulations have been accomplished for spacer with mixing vane and spacer without mixing vane in an annular channel by using commercial CFD (Computational fluid dynamics) code ANSYS Fluent. The present investigation represents the comparative study for spacer with mixing vane and spacer without mixing vane effects on heat transfer and flow field characteristics in a downstream direction for mass flow-rate 0.41469 kg/s and heat flux 160 kW/m^2. The results indicate that spacer with mixing vane has notable influence on heat transfer performance and flow field characteristics downstream of mixing vane spacer as compared to spacer without mixing vane. Wall temperature fall and increase of coefficient of heat transfer are significantly greater adjacent to spacer downstream. Spacer influence in the improvement of the heat transfer is noted up to distance X/D = 40 downstream and then flow is found as fully developed.

Cite this article as: Dhurandhar SK, Sinha SL, Verma SK. Numerical simulation to study mixing vane spacer effects on heat transfer performance of supercritical pressure fluid in an annular channel. J Ther Eng 2023;9(6):1428−1441.

INTRODUCTION

Spacer grids are an essential component of rod bundles and are placed along the fuel channels. Spacer grids are arranged to provide structural support and the necessary gap between the rods in the nuclear fuel assembly. Mixing vanes are affixed to the upper part of the grid spacer in the downstream flow direction of nuclear fuel channels. Mixing vane grid spacer functions as flow blockage in the bundle of fuel rods and cause an enhanced rate of turbulent mixing of

***Corresponding author.**
*E-mail address: satishdhurandhar@gmail.com

This paper was recommended for publication in revised form by Regional Editor Tolga Taner

coolant and improved performance of heat transfer. In the nuclear reactor core, the fuel channels are surrounded by the coolant and it flows axially upward in between the fuel rod bundle. During the flow between rods in a fuel bundle, coolant lowers the wall temperature (Cladding temperature) of the fuel rod and it performs as a shield from radiation that is emitted due to the fission process in the reactor core. Due to mixing vane grid spacer, the flow phenomena such as mixing, flow structure, and flow distribution of working fluid (coolant) become complicated within subchannels of fuel rod assembly, and therefore the detailed study for spacer with mixing vane effects on heat transfer performance and flow features of fluid is a vital field for the nuclear industry in the view of optimal design of spacer grid with mixing vane of rod bundle for safe and reliable functioning of the nuclear reactor core.

In 2002, under research and development work; the Generation IV International Forum chose the SCWR (Supercritical pressure water-cooled reactor) concept out of six concepts of a nuclear reactor [1]. Power plants based on SCWR have benefits of the higher thermal efficiency and simple system due to their operation at high temperature and pressure as compared to power plants work on light water-cooled reactors [2]. The purpose designing of the SCWR is to control the wall temperature of the fuel rod to confirm the safety of the reactor core, and using mixing vane spacer grid is a constructive method to decrease wall surface temperature of rods in the assembly of fuel rod [3].

Numerous computational and experimental studies have been accomplished in the previous years to study the spacer with mixing vane influences on heat transfer performance and flow field characteristics in the downstream flow direction of fuel rods. Gang et al. [4] experimentally examined the heat transfer performance at the supercritical condition in annular channel by a spacer of spiral shape. The measurements were conducted for channel wall temperature at supercritical pressure and observed that the wall temperature reduces drastically at the spiral-shaped spacer location. Numerical investigations were conducted for heat transfer analysis of water due to wrapped wire in the single rod by Zhu and Laurien [5] and noticed that the heat transfer coefficient was improved downstream to the wrapped wire. Analyses on convective heat transfer in tubes were performed experimentally for supercritical pressure of water by Yamagata et al. [6]. They observed that the coefficient of heat transfer was notably enhanced and maximum at the pseudo-critical temperature. Swenson et al. [7] worked on the analysis of forced convection heat transfer for supercritical water in tubes and observed to be in increased heat transfer rate at pseudo critical region. Zhu et al. [8] numerically analyzed the effect of split type mixing vane spacer on heat transfer of supercritical water in rod bundle having hexagon structure and reported that spacer with mixing vane has significant influence on the heat transfer in the downstream direction from spacer grid. Effects of spacer on wall temperature and local heat transfer of R134a (supercritical) in vertical flow annular channel were studied numerically by Xiao et al. [9]. They revealed that the surface temperature of the rod was reduced and the corresponding heat transfer coefficient increased remarkably by the presence of spacer. Holloway et al. [10] performed experimental measurements to analyze heat transfer of single-phase fluid under subcritical pressure in a 5x5 rod bundle with and without mixing vane support grid and observed that the Nusselt number is highest at just behind the grid support in the rod bundle. They suggested a correlation for Nusselt number ratio in rod bundle without mixing vane, which is given as:

$$\frac{Nu}{Nu^*} = 1 + 6.5\varepsilon^2 e^{-0.8(\frac{X}{D_h})} \quad (1)$$

Where Nu and Nu* denotes the Nusselt number for with and without spacer grid in rod bundle respectively, ε refers to the blockage ratio (the ratio between the obstructed cross-section area and the area of the unobstructed fluid domain), x is the distance taken in axial flow direction behind support grid and D_h represents the hydraulic diameter. Bhattacharjee et al. [11] numerically studied for influences of spacer grid mixing vane on pressure & hydraulic behavior in an annular channel and reported that the mixing vane and grid spacer have a combined influence on flow acceleration and swirl flow pattern downstream to spacer grid. Miller et al. [12] developed a correlation for single-phase heat transfer enhancement of steam at subcritical pressure in a 7x7 rod bundle with a spacer grid. They used this correlation for Reynolds number (Re) ranges from 8000 to 30000 [Eq. (2)].

$$\frac{Nu}{Nu^*} = 1 + 465.4Re^{-0.5}\varepsilon^2 e^{-7.31\times10^{-6}Re^{1.15}(\frac{X}{D_h})} \quad (2)$$

Effects of grid spacer mixing vane on the hydraulic and thermal performance of fuel rod assembly were studied through the experimental and numerical method by Ikeda [13]. It is revealed that the acquired information is useful for the development of spacer grid design. Experimental measurements were conducted by Yao et al. [14] in spacer grid rod bundle and used a correlation in enhanced heat transfer performance downstream to grid support. The correlation is given as:

$$\frac{Nu}{Nu^*} = 1 + 5.55\varepsilon^2 e^{-0.13(\frac{X}{D_h})} \quad (3)$$

Wang et al. [15] numerically worked on the design of a grid spacer mixing vane of the fuel rod assembly. Parametric studies for mixing vane design such as vane angle, vane length, etc. were made by them and reported that vane angle has significant effects on pressure drop and heat transfer performance. Tanase and Groeneveld [16] executed experimental observations to study the flow

obstructions' effects on heat transfer performance of single-phase R134a at subcritical pressure. Based on their experimental measurements, they developed a correlation for the prediction of heat transfer, which is given as:

$$\frac{Nu}{Nu^*} = 1 + 3.58 \times 10^{-5} Re\varepsilon^{\{0.47\ln(Re)-3.32\}} e^{-0.13(\frac{X}{D_h})} \quad (4)$$

Experimental measurements were conducted by Eter al. [17] for studying the heat transfer performance of CO_2 at supercritical pressure in tubes with and without consideration of flow obstructions. A remarkable improvement in heat transfer was found at the location of flow obstacles. Experimental measurements were conducted by Qu et al. [18] to study the lateral flow and pressure drop in a 5x5 rod bundle by a support grid mixing vane. Pressure transmitters were used for measurement in sub channels. Pressure loss was analyzed through resistance models. Influences of vane angles on heat transfer were studied numerically by Yang et al. [19] in a 3x3 rod arrangement and they suggested an optimal angle of vane for spacer grid mixing vanes design. Huang et al. [20] used the CFD method to study the heat transfer of water in a rectangular channel with round blisters and observed that blister increases the resistance during fluid flow inside the channel and boiling take place at the area close to the blister's edges. Heat transfer analysis in the 5x5 rod arrangement was conducted numerically by Wang et al. [21]. They considered the spacer grid mixing vanes for their analysis. Ahmadpour et al. [22] numerically studied the outside magnetic field effect on the natural convection of a metal (molten) inside the vertical annulus and revealed that the outside magnetic field causes a reduction in convective heat transfer. Experimental and CFD methods were used by Verma and Sinha [23] to study the heat transfer characteristics in an isolated room. They used Realizable, RNG, and Standard k-ε models for CFD simulations. Xiong et al. [24] experimentally examined the mixing vane effects on flow performance in a 5x5 rod bundle. They conducted measurements by using particle image velocimetry technique to acquire data of flow field in rod bundle assembly. Furthermore, the comparison of the present study with the related published work has been given in Table1.

In summary, the spacer/spacer grid with and without mixing vane has significant effects on the heat transfer and hydraulic characteristics of the fluid downstream to support the grid of nuclear fuel channels. Spacer (without mixing vane) effects for the analysis to heat transfer characteristics in annular channel have been studied by many researchers in the past. Analysis of spacer with mixing vane effects on heat transfer and flow characteristics of supercritical pressure fluid in an annular channel is a novel work. This paper presents the numerical studies of mixing vane spacer effects on heat transfer of R134a at supercritical pressure 4.5 MPa in vertical annular flow. Simulations were performed by ANSYS Fluent for the spacer of 0.38 blockage ratio with and without mixing vane in annular channel. The turbulent characteristic of flow has been modeled by using the turbulence model as SST k-ω. The detailed comparative study for spacer with mixing vane and spacer without mixing vane effects on flow field characteristics and downstream heat transfer have been accomplished with the flow conditions of mass flow rate and heat flux as 0.41469 kg/s and 160 kW/m^2, respectively. In this study, the existence of mixing vane on spacer provides benefits of enhanced flow characteristics and heat transfer as compared to spacer without mixing vane in annular channel as proved by literature. Therefore, the proposed study will support the interpretation of improved heat transfer and flow phenomena in annular channel with vanes. Also, the data from CFD results of present study will support the development and design of new spacer vane in annular channel.

MATERIALS AND METHODS

Mathematical Model

In the present analysis, spacer with mixing vane influences on heat transfer has been studied in 3-dimensional vertical annular flow by using CFD methodology which solves the mathematical model numerically during simulation. The finite volume method (FVM) is used for numerical simulations in the CFD code (ANSYS Fluent). The partial differential governing equations are converted into algebraic equations by discretization. This discretization is based on the finite volume formulation. Finite volume denotes the small volume surrounding each node point on a mesh. Unstructured mesh can also be easily formulated by FVM. The mathematical model comprises governing equations and turbulence models which are as given below:

Governing equations:

Continuity equation

$$\frac{\partial(\rho u_i)}{\partial x_i} = 0 \quad \text{(Index form)}$$

$$\nabla.\vec{u} = 0 \quad \text{(Vector form)}$$

$$\frac{\partial u}{\partial x} + \frac{\partial v}{\partial y} + \frac{\partial w}{\partial z} = 0 \quad \text{(Expanded form)}$$

Reference or characteristic quantities: Length- L, Flow velocity- U, Time- L/U.

Non-dimensional variables:

$$x^* = \frac{x}{L},\ y^* = \frac{y}{L},\ z^* = \frac{z}{L}, u^* = \frac{u}{U}, v^* = \frac{v}{U},\ w^* = \frac{w}{U}$$

By putting the above non-dimensional variables in the continuity equation, we have

Table 1. Comparison of the present study with the related published work

Name of Researchers	Methods (Analytical / CFD / Experimental)	Geometry	Dimensions/ Parameters	Fluid Considered	Conclusions/Remarks/ Significance
Wang et al. [2]	Experimental and Numerical analysis	Vertical annular channel with spiral spacer	Channel length = 1400 mm, hydraulic diameter = 12 mm, Mass fluxes = 350 to 1000 kg/m^2, Pressures = 23 to 28 MPa	Supercritical Water	Analysis of the augmented effect of spiral-shaped spacer on heat transfer.
Gang et al. [4]	Experimental study	Vertical annular channel with spiral spacer	Channel length = 1400 mm, hydraulic diameters = 8 & 12 mm, Pressures = 23 to 28 MPa, Inlet fluid temperature = 275 ^{0}C to 400 ^{0}C	Supercritical Water	Study of heat transfer on the channel due to spiral-shaped spacer.
Zhu et al. [8]	Numerical analysis (CFD - STAR CCM+)	Rod bundle (Hexagon shape) with mixing vane spacer grid	Blockage ratio = 0.38 and Pitch/Diameter =1.12, Reynolds number (Re) = 50,000 and 100,000	Supercritical Water	Effect of split type mixing vane spacer grid on heat transfer.
Xiao et al. [9]	Numerical analysis (CFD - ANSYS Fluent)	Annular channel with spacer	Blockage ratio = 0.2, 0.3 & 0.4, Hydraulic diameter = 6 mm	Supercritical R134a	Heat transfer analysis was performed on the channel.
Holloway et al. [10]	Experimental study	5 x 5 rod bundle (Spacer Grid with Split vane pair)	Blockage ratio = 0.2, 0.31, 0.4, 0.43, 0.47 and Re = 28000 & 42,000	Water	Heat transfer and pressure drop analysis in rod bundle.
Tanase and Groeneveld [16]	Experimental	Tube with flow obstacle (spacer) of annular shape	Blockage ratio = 0.264 & 0.3, Re = 14200, 28300,56000 & 97000	R134a	Flow obstacle effects on heat transfer were analyses.
Wang et al. [21]	Numerical analysis	5 x 5-rod bundle with mixing vane spacer grid	Hydraulic diameter = 24.27 mm, Pitch/ Diameter = 1.3, Re = 50250	Water	Influences of spacer with mixing vane on hydraulic and thermal characteristics.
Zhang et al. [25]	Experimental	circular tube	Tube diameter = 7.6 mm, pressures = 4.3 to 4.7 MPa, fluid temperature = 71 to 115 ^{0}C, heat fluxes = 20 to 180 kW/m^2	Supercritical R134a	Analysis of wall temperature and coefficient of heat transfer for different heat and mass fluxes.
Cheng et al. [26]	Numerical analysis	Vertical tubes	Tube diameters = 8 & 22.8 mm, lengths = 2200 & 5016 mm, Re for water = 43335, Re for CO_2 = 96075	Supercritical Water and Supercritical CO_2	Radial distributions of velocity and turbulent kinetic energy were studied for different axial locations in tubes.
Present study	Numerical analysis	Annular channel (Spacer with and without mixing vane)	Channel length = 1000 mm, Blockage ratio = 0.38, Hydraulic diameter = 6 mm, heat flux = 160 kW/m^2, Re = 100000	Supercritical R134a	Comparative analysis for the spacer effects without mixing vane (i.e. spacer only) and spacer with mixing vane on flow performance and heat transfer.

$$\frac{U}{L}\left[\frac{\partial u^*}{\partial x^*}+\frac{\partial v^*}{\partial y^*}+\frac{\partial w^*}{\partial z^*}\right]=0$$

$$\frac{U}{L}\left[\nabla^*.\vec{u}^*\right]=0$$

$$\nabla^*.\vec{u}^*=0$$

Generalized form

$$\frac{\partial(\rho u_i)}{\partial x_i}=0 \quad (5)$$

Momentum equation

$$\frac{\partial u}{\partial t}+(u\,.\,\nabla)\,u=-\frac{1}{\rho}\nabla p+\nu\nabla^2 u+g$$

Non-dimensional variables:

$$x^*=\frac{x}{L},\ y^*=\frac{y}{L},\ z^*=\frac{z}{L},u^*=\frac{u}{U},v^*=\frac{v}{U},\ w^*=\frac{w}{U},t^*=t\frac{U}{L}$$

$$\nabla^*=\hat{\imath}\frac{\partial}{\partial x^*}+\hat{\jmath}\frac{\partial}{\partial y^*}+\hat{k}\frac{\partial}{\partial z^*}$$

Where, ∇^* is an operator.

$$\nabla^*=L\hat{\imath}\frac{\partial}{\partial x}+L\hat{\jmath}\frac{\partial}{\partial y}+L\hat{k}\frac{\partial}{\partial z}$$

$$\nabla^*=L[\hat{\imath}\frac{\partial}{\partial x}+\hat{\jmath}\frac{\partial}{\partial y}+\hat{k}\frac{\partial}{\partial z}]$$

$$\nabla^*=L\nabla$$

$$p^*=\frac{p+\rho gz}{\rho u^2}$$

By substituting the above non-dimensional variables in the momentum equation, we have

$$\frac{\partial u^*}{\partial t^*}+(u^*\,.\,\nabla^*)\,u^*=-\nabla^* p^*+\frac{1}{Re}\nabla^{*2}u^*+\frac{1}{Fr^2}g$$

Where Reynolds Number, $Re=\frac{\rho UL}{u}$

Froude Number, $Fr=\frac{U}{\sqrt{gL}}$

Generalized form

$$\frac{\partial(u_i)(u_j)}{\partial x_j}=g_i-\frac{1}{\rho}\frac{\partial(P)}{\partial x_i}+\frac{1}{\rho}\frac{\partial}{\partial x_j}\left[\mu\left(\frac{\partial(u_i)}{\partial x_j}+\frac{\partial(u_j)}{\partial x_i}\right)-\overline{\rho u_i' u_j'}\right] \quad (6)$$

Energy equation

$$\frac{\partial T}{\partial t}+u_j\frac{\partial T}{\partial x_j}=\frac{k}{\rho c_p}\frac{\partial^2 T}{\partial x_j\partial x_j}$$

Non-dimensional variables:

$$u_j{}^*=\frac{u}{U}\ ,\ x_j{}^*=\frac{x_j}{L}\ ,t^*=\frac{t}{t_0},T^*=\frac{T-T_0}{T_1-T_0}$$

Where, T_1 and T_0 are reference temperatures.

By substituting the above non-dimensional variables in the energy equation, we have

$$\frac{\partial(T^*(T_1-T_0)+T_0)}{\partial(t^*t_0)}+u_j{}^*\,U\frac{\partial(T^*(T_1-T_0)+T_0)}{\partial(\,x_j{}^*L)}=\frac{k}{\rho c_p}\frac{\partial^2(T^*(T_1-T_0)+T_0)}{\partial(\,x_j{}^*L)\partial(\,x_j{}^*L)}$$

Here T_1, T_0, L, and t_0 are constants.

$$\frac{(T_1-T_0)}{t_0}\frac{\partial T^*}{\partial t^*}+\frac{U\,(T_1-T_0)}{L}u_j{}^*\frac{\partial T^*}{\partial x_j{}^*}=\frac{k}{\rho c_p}\frac{(T_1-T_0)}{L^2}\frac{\partial^2 T^*}{\partial x_j{}^*\partial x_j{}^*}$$

Divide the above equation by $\frac{U\,(T_1-T_0)}{L}$

$$\frac{L}{Ut_0}\frac{\partial T^*}{\partial t^*}+u_j{}^*\frac{\partial T^*}{\partial x_j{}^*}=\frac{k}{\rho c_p}\frac{1}{UL}\frac{\partial^2 T^*}{\partial x_j{}^*\partial x_j{}^*}$$

Let, Reynolds Number, $Re=\frac{\rho UL}{u}$

Prandtl Number, $Pr=\frac{\rho c_p}{k}$

Strouhal Number, $St=\frac{L}{Ut_0}$

Hence,

$$st\ \frac{\partial T^*}{\partial t^*}+u_j{}^*\frac{\partial T^*}{\partial x_j{}^*}=\frac{1}{Pr}\frac{1}{Re}\frac{\partial^2 T^*}{\partial x_j{}^*\partial x_j{}^*}$$

Generalized form

$$\frac{\partial}{\partial x_i}[(u_i)(\rho E+P)]=\frac{\partial}{\partial x_i}[K\,(\frac{\partial T}{\partial x_i})+(u_j)(\tau_{ij})] \quad \mathbf{(7)}$$

Turbulence model - The SST k-ω turbulence model comprises the two transport equations, one is for transport of k (Turbulence kinetic energy) and another is for transport of ω (specific dissipation rate of k). These two transport equations are given as:

$$\frac{\partial}{\partial t}(\rho k)+\frac{\partial}{\partial x_i}(\rho k u_i)=\frac{\partial}{\partial x_j}(\Gamma_k\frac{\partial k}{\partial x_j})+G_k-Y_k+S_k \quad (8)$$

$$\frac{\partial}{\partial t}(\rho\omega)+\frac{\partial}{\partial x_i}(\rho\omega u_i)=\frac{\partial}{\partial x_j}(\Gamma_\omega\frac{\partial\omega}{\partial x_j})+G_\omega-Y_\omega+D_\omega+S_\omega \quad \mathbf{(9)}$$

Notations and values of constants used in the transport equations for present simulations have been fetched by ANSYS guide [27].

Computational Geometry and Boundary Conditions

Figure 1 represents the computation geometry used in numerical simulations, which is a vertical annulus channel with a mixing vane spacer. The length, inner diameter, and outer diameter of the vertical annular channel are taken as 1000 mm, 19 mm, and 25 mm respectively. The spacer of 0.38 blockage ratio is placed at the mid-portion of the channel and in the downstream direction of an annular channel; the mixing vanes are attached at the upper part of the spacer, which can be seen with the help of Figure 2. The present computational geometry (annular channel) is having 6 mm of hydraulic diameter and the length of spacer used is taken as 10 mm. The flow direction is axially upward in an annular flow channel. In this investigation, numerical simulations for a spacer with mixing vane and spacer without mixing vane (i.e. spacer only) in an annular channel have been performed for analysis.

For numerical simulations in the computational geometry, mass flow rate, the hydraulic diameter, turbulence intensity, and inlet temperature of fluid are defined as the inlet boundary conditions of the fluid domain. Constant pressure is applied as an outlet boundary condition. Smooth and no-slip boundary conditions are set under the momentum equation to all the walls of the computational geometry. Constant heat fluxes are applied as boundary parameters at inner and outer walls. R134a is considered a working fluid and its properties have been taken at supercritical pressure from the NIST databank. Reynolds number of fluid flow for the current study is calculated as 100000.

Table 2. Boundary conditions used of CFD simulations in the annular channel

Boundary parameters	Property with its value
Inlet	Mass flow rate = 0.41469 kg/s
	Hydraulic diameter = 0.006 m
	Turbulence Intensity = 4 %
Outer wall	Heat flux (Constant) = 160 kW/m^2
Outlet	Pressure = 4.5 MPa
Inner wall	Adiabatic wall

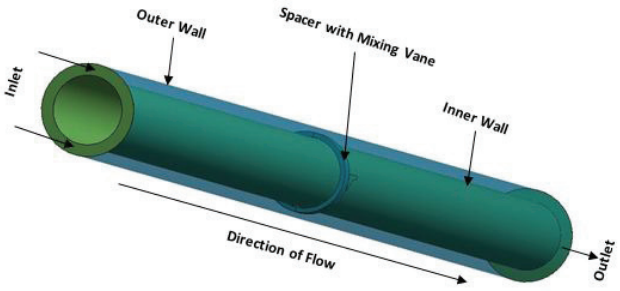

Figure 1. Annular channel - computational geometry.

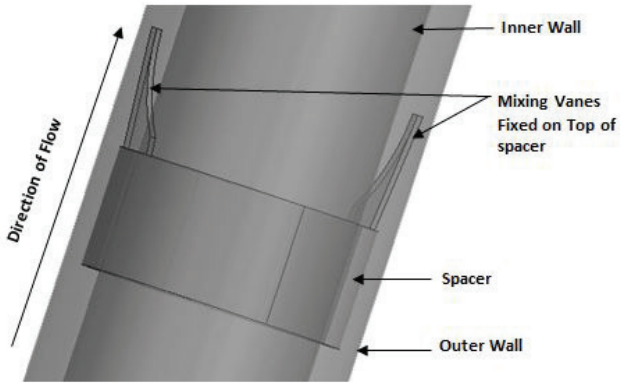

Figure 2. Annular channel showing mixing vanes with spacer.

Table 2 represents the detail of boundary conditions used for CFD simulations.

Numerical Model Validation

Validation of CFD results (with RNG k-ε, Standard k-ε, and SST k-ω) has been conducted for supercritical R134a in the vertical circular tube against experimental data [25]. The length and inner diameter of circular tube were taken as 2300 mm and 7.6 mm, respectively. Turbulence models were examined for parameters - mass flux, heat flux and supercritical pressure (of R134a) as 600 kg/m2s, 30 kW/m^2, and 4.3 MPa, respectively. Figure 3 represents wall temperature variation against specific enthalpy. Wall temperature gradually increases with specific enthalpy and CFD result for SST k-ω gives better agreement with experiment. Hence, further CFD simulations were performed by turbulence model of SST k-ω. Additionally; in previous research works [26, 28, 29], the various turbulence models have been

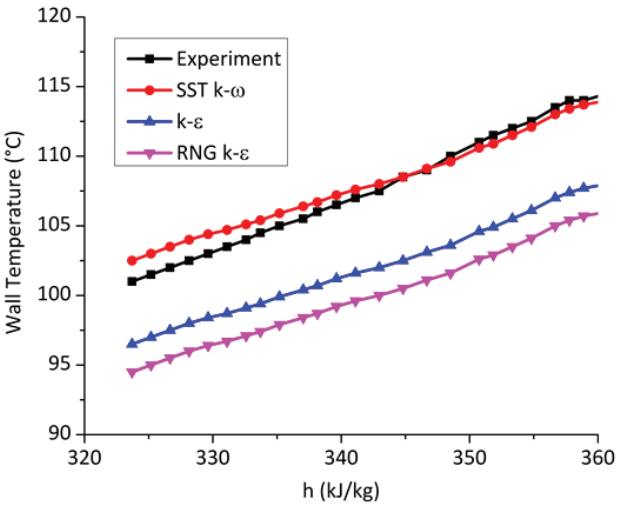

Figure 3. Comparison of experimental data and CFD result in upward flow circular tube.

studied by researchers for the prediction of heat transfer performance of supercritical fluid flows in vertical channels and they reported that heat transfer of fluid flows at supercritical condition are predicted more accurately with SST k-ω turbulence model. Also, the SST k-ω turbulence model had been applied in past research through simulation investigations [30-33] for the analysis of flow field and heat transfer characteristics for spacer grids mixing vane.

Figure 4(a) shows a mesh independence test, which has been conducted on a validation model for the mass flux 2000 kg/m^{2}s, heat flux 100 kW/m^2, 4.5 MPa pressure and the turbulence model as SST k-ω. The validation model is an annular channel with spacer of 0.3 blockage ratio and the dimensions of this channel are the same as mentioned in computational geometry. Three meshes of different element counts such as mesh-A of 1.5 million, mesh-B of 1.4 million, and mesh-C of 1.0 million have been generated. The wall temperature distribution against specific enthalpy are studied for these three meshes at X/D=0 of annular channel. Basis on a comparison of wall temperature against specific enthalpy, mesh-B has been selected for the numerical model validation [Refer-figure 4(a)].

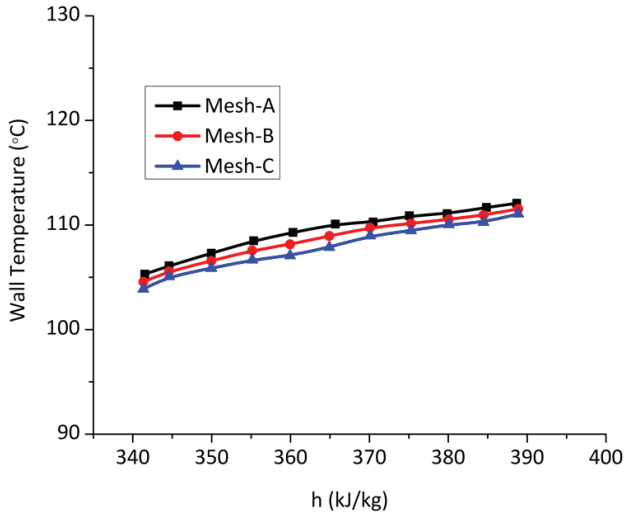

Figure 4 (a). Mesh independence test of validation model.

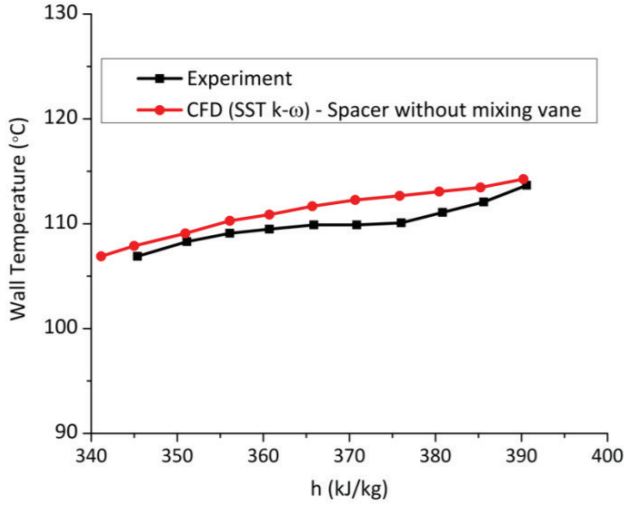

Figure 4 (b). Numerical model validation with experimental work.

Furthermore, numerical model validation has been performed for spacer without mixing vane in annulus channel against experimental data [9]. The dimensions of geometry are the same as mentioned in the above section of computational geometry. Validation was performed for parameters-mass flux 2000 kg/m^{2}s, heat flux 100 kW/m^2, 4.5 MPa pressure, and spacer blockage ratio as 0.3 in annulus channel. Figure 4(b) shows comparison of CFD result for the spacer without mixing vane against experimental data at X/D=7.5 downstream to the spacer. Wall temperature & specific enthalpy are drawn on the ordinate and abscissa, respectively. Figure represents that the CFD result for SST k-ω gives better agreement with experiment.

Mesh Generation of the Proposed Model

In this analysis, mesh independence study has been conducted in a vertical annular channel with mixing vane spacer for flow conditions as mass flow rate 0.41469 kg/s, heat flux 160 kW/m^2, and 4.5 MPa system pressure. Three different sizes of meshes (mesh1 of 1.7 million, mesh 2 of 1.6 million, and mesh 3 of 1.4 million elements count) have been created by distinct mesh alterations on mixing vanes and spacer of computation fluid domain with retaining scale factor as same. Also, adjacent to the wall, the y^+ is maintained smaller than 1.0. For the above three meshes, the tangential velocity radial distribution at 450 mm from inlet of channel is given in figure 5. On comparing of the tangential velocity in the radial direction (Refer to figure 5), mesh 2 has been selected for further CFD simulations.

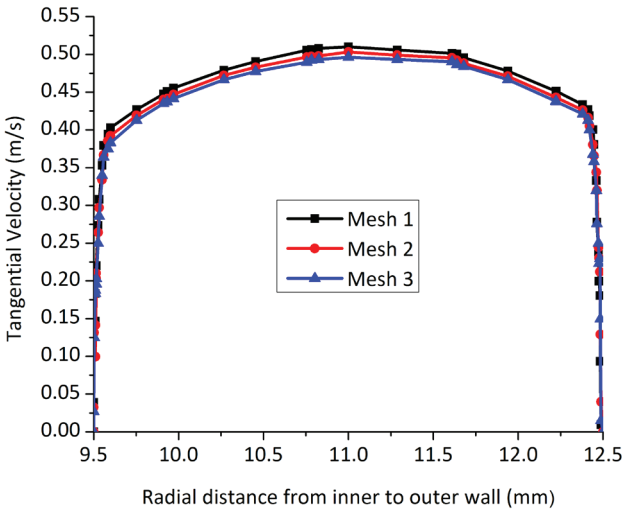

Figure 5. Mesh independence test.

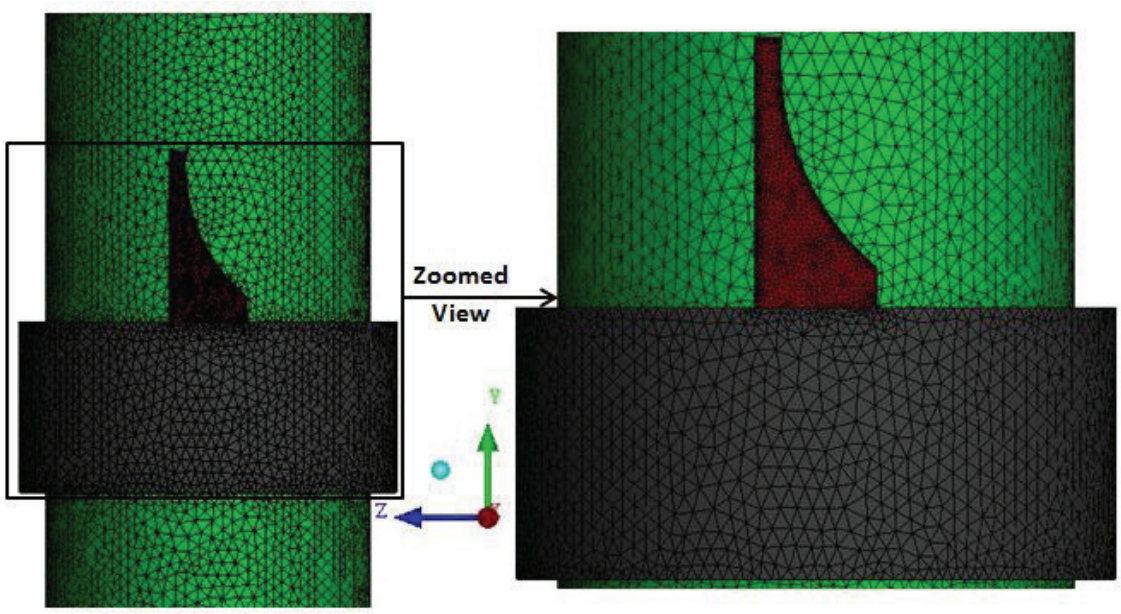

Figure 6. (a) Surface mesh of mixing vane spacer and inner wall.

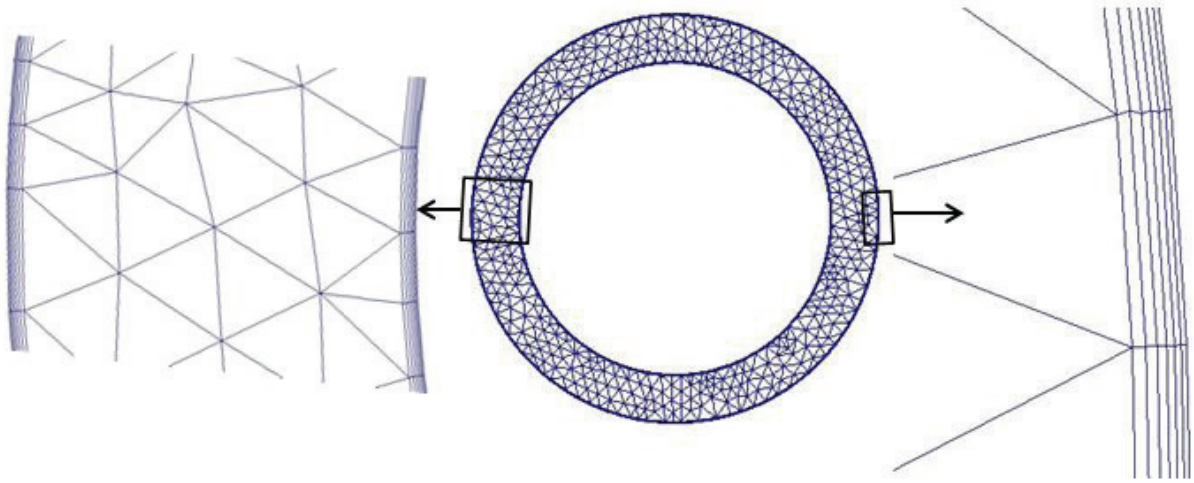

Figure 6. (b) Mesh at inlet cross section.

Figure 6 (a) shows the surface mesh (tetrahedron type element) of mixing vane spacer and inner wall portion. Figure 6 (b) shows the mesh of the inlet cross-section. The prismatic elements layers with extension ratio as 1.2 have been generated near the wall.

RESULTS AND DISCUSSION

Mixing Vane Spacer Effects on the Heat Transfer Performance

In this section, the comparative study for influences of spacer without mixing vane (i.e. spacer only) and spacer with mixing vane on the heat transfer performance of R134a (on supercritical pressure) within vertical flow annular channel has been made. Results are obtained for the spacer of blockage ratio 0.38, mass flow-rate 0.41469 kg/s, heat flux 160 kW/m^{2,} and 4.5 MPa system pressure. Figure 7 shows wall temperature variation in the axial flow direction. Wall temperature variation is taken on the ordinate and non-dimensional (X/D) distance by the abscissa, where, D represents the hydraulic diameter and X is the distance taken in axial flow direction. It has been observed from the figure that wall temperature fall is significant at spacer point. Wall temperature fall is more which is around 2.5^{0}C adjacent spacer downstream while considering spacer

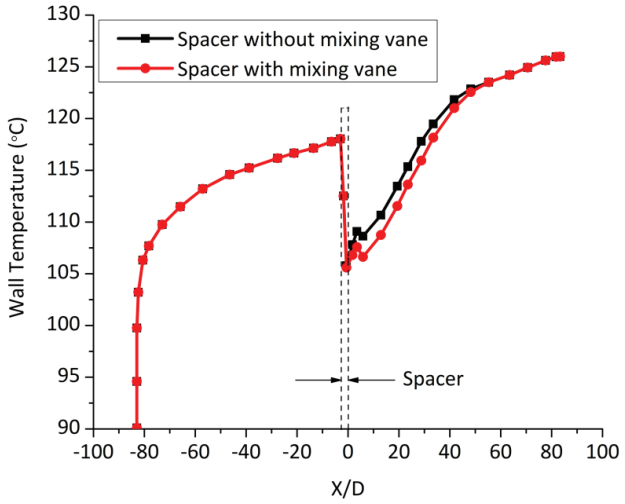

Figure 7. Wall temperature.

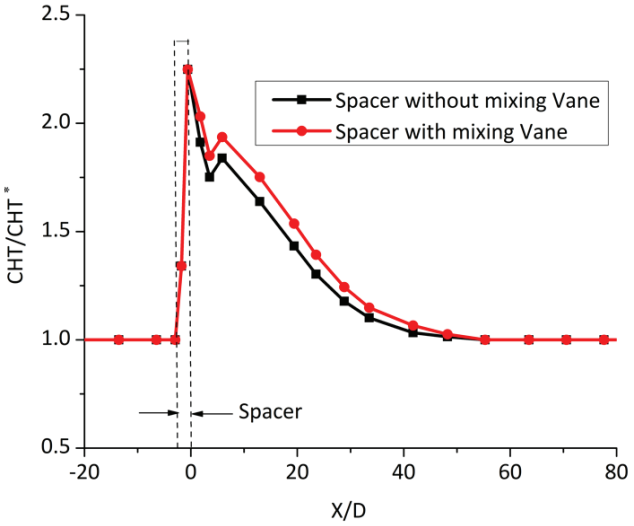

Figure 9. Ratio of coefficient of heat transfer.

with mixing vane as compared to the case of spacer without mixing vane in channel. The existence of mixing vane causes add on turbulence mixing and therefore the more reduction has been observed in wall temperature of the channel.

Figure 8 shows coefficient of heat transfer (CHT) distribution on the channel axial length. The result represents that the augmentation in CHT is remarkable within the spacer point. The existence of spacer functions as a flow obstruction inside the channel. Spacer reduces the flow area which causes a significant increment in the velocity of flow. This increased flow velocity causes the augmentation in the CHT at spacer point. Due to the existence of mixing vane, the enhancement in CHT is greater near downstream to a spacer for the case of the spacer with mixing vane as compared to the spacer without mixing vane in channel.

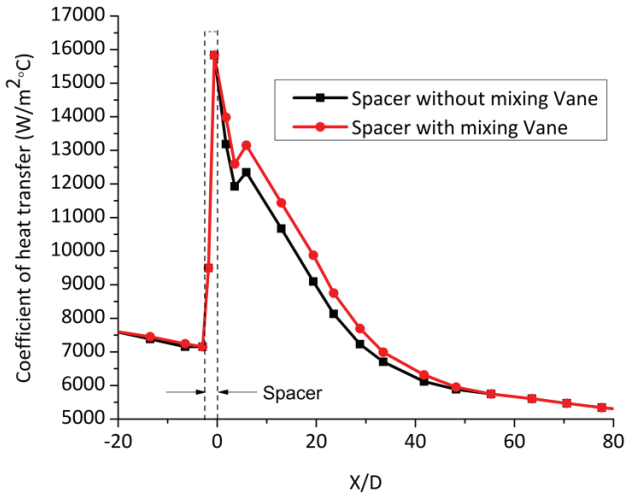

Figure 8. Coefficient of heat transfer.

Ratio between coefficient of heat transfer (CHT/CHT*) against non-dimensional channel axial length is represented in figure 9. Where, CHT* represents the CHT for the case of without spacer annular channel. Figure 9 also represents that the CHT/CHT* has been enhanced greatly within the spacer location and at spacer location; the CHT/CHT* is found to be maximum which is around 2.2. For specified flow conditions in the present study, the spacer influence in improvement of the CHT/CHT* is observed up to the X/D = 40 in downstream, and then flow is found to fully developed. Also, the existence of mixing vane causes the add on turbulence mixing and hence the CHT/CHT* is greater in adjacent spacer downstream while considering the spacer with mixing vane as compared to the spacer without mixing vane in channel.

Mixing Vane Spacer Effects on the Flow Characteristics

The results discussed in this section are obtained for the spacer of blockage ratio 0.38, mass flow-rate 0.41469 kg/s, heat flux 160 kW/m^2, 4.5 MPa system pressure, and the calculated flow Reynolds number (Re) as 100000 in the annular channel. The relative discussion has been made for the influences of spacer without mixing vane (i.e. spacer only) and spacer with mixing vane on flow field characteristics of R134a (on supercritical pressure) within vertical flow annular channel. Spacer with and without mixing vane effects on axial velocity and static pressure distributions along the length of the annular channel are represented in figures 10 & 11, respectively. Axial velocity and static pressure distributions have been illustrated along channel length which is at a distance of 0.65 mm from outer wall. It has been observed from the figure 10 that axial velocity increased significantly within the spacer region. Reduced flow area at spacer point is the cause of increased velocity. Axial velocity was found to be peak which is about 4.2 m/s at the spacer point. Improve in velocity is observed as higher at the zone,

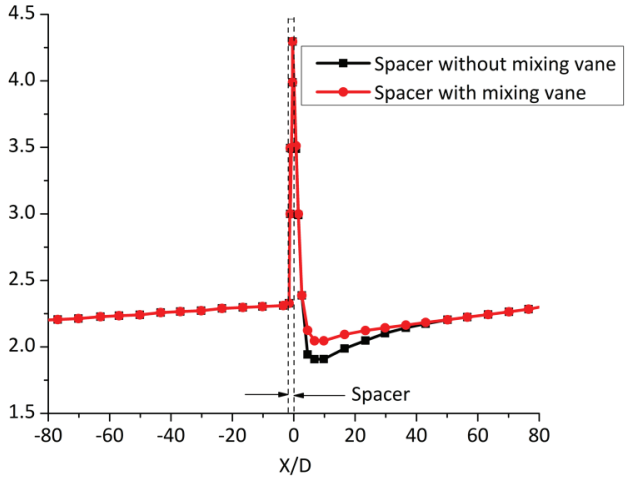

Figure 10. Axial velocity distribution.

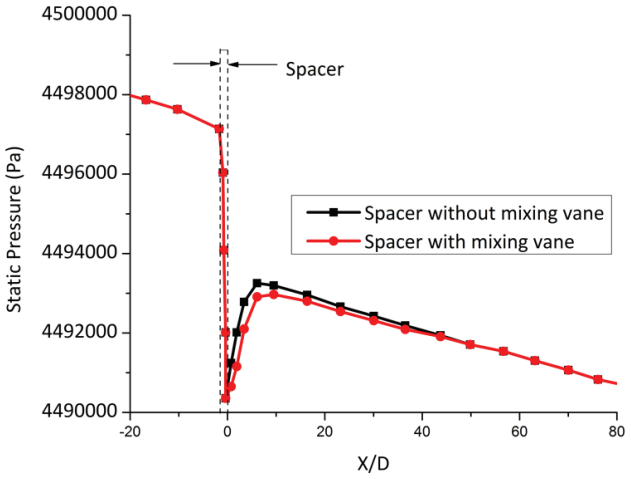

Figure 11. Static pressure distribution.

adjacent to spacer in downstream while considering the spacer with mixing vane as compared to the spacer without mixing vane in channel. Figure 11 illustrates the notable fall in pressure within spacer point. Fall in pressure is because of the existence of spacer which decreases the flow area. Fall in pressure is observed as more adjacent to spacer in downstream while considering the spacer with mixing vane as compared to the spacer without mixing.

Figure 12 and figure 13 illustrate the influences of the spacer with mixing vane and without mixing vane on radial variations of velocity and turbulent kinetic energy (TKE). Figure 12 illustrates that velocity adjacent to wall (outer) enhanced greatly near behind to spacer (X/D = 2) because of the spacer influence. Beyond Downstream to X/D = 2, the velocity adjacent to wall (outer) falls gradually and later, the flow is observed to be fully developed in further downstream (X/D= 20) of the channel. Also; due to the mixing vane, at these three considered locations in downstream the velocity magnitude is higher while considering the spacer with mixing vane as compared to the spacer without mixing vane in channel.

It has been observed from the figure 13 that the turbulent kinetic energy (TKE) is greater at closest location to spacer (X/D=2) than the downstream locations (X/D=5 &20). Higher turbulent kinetic energy is because of spacer

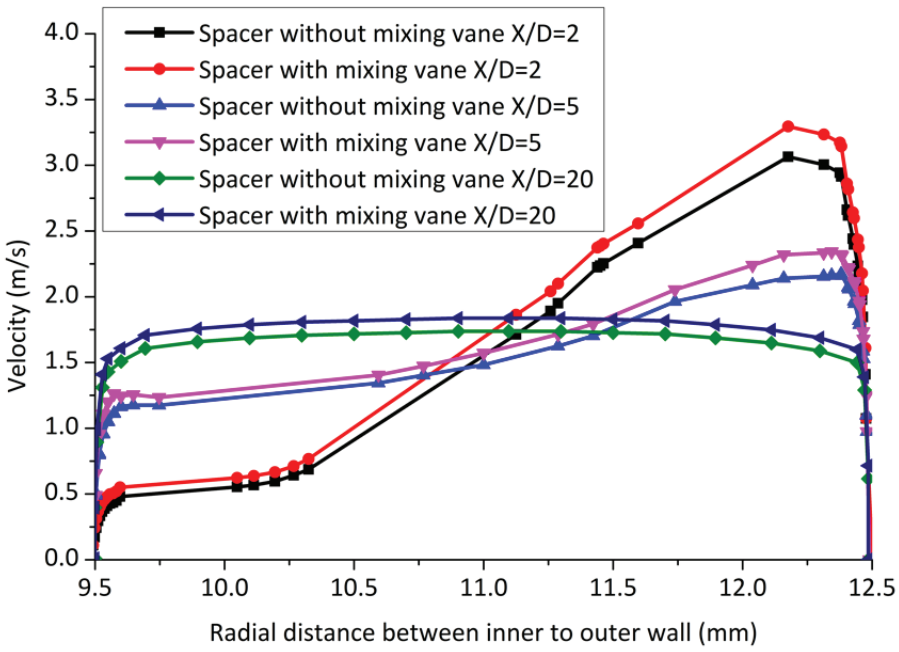

Figure 12. Radial distribution of velocity.

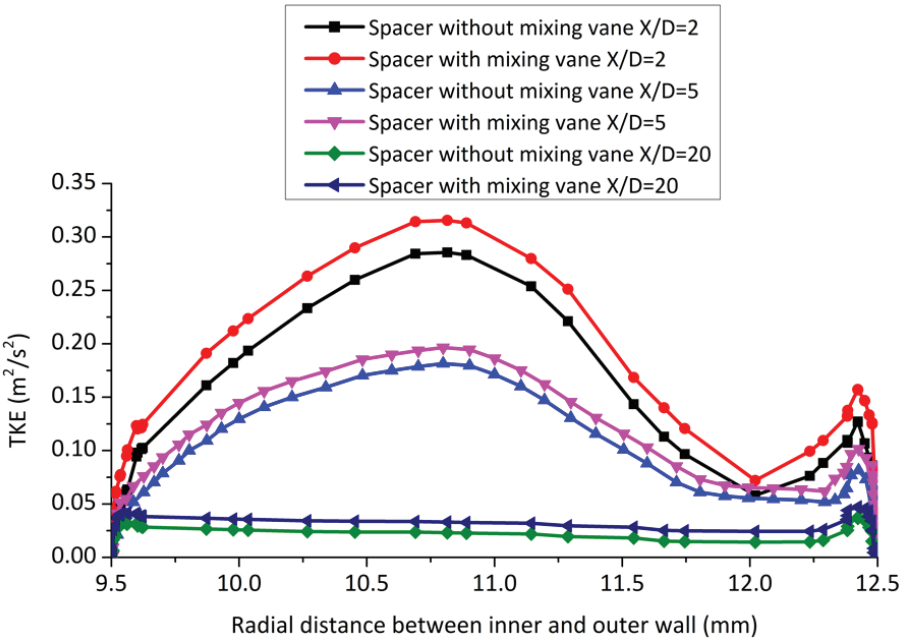

Figure 13. Radial distribution of turbulent kinetic energy (TKE).

influence which causes the heat transfer boost in adjacent downstream of spacer. It can also be viewed from figure 13 that the turbulent kinetic energy again improves adjacent to outer wall because of reduced flow area caused by a spacer. Mixing vane causes the TKE boost and therefore, at these three considered locations in downstream the TKE is greater while considering the spacer with mixing vane as compared to the spacer without mixing vane in channel.

Figure 14 shows velocity contours at different positions (i.e. X/D = 0, 1, 3 and 40) in axial flow direction. The velocity close to outer wall noticed as maximum (around 4.3 m/s) at position X/D = 0. This maximum velocity is because of the minimum flow passage at spacer, which acts as flow obstruction. Velocity decreases gradually downstream to the spacer (X/D =1, 3) and flow gets fully developed in far downstream (X/D =40).

Comparison - CFD Results and Correlations Data

The comparison of correlations data with present CFD results are shown in figure 15. The equations of correlations have been given in the introduction section by equations (1)-(4). Researchers were developed these correlations for single phase fluid. CFD results for comparison were produced with Reynolds number and spacer blockage as 100000 and 0.38, respectively. Figure 15 represents Nusselt number ratio (Nu/Nu^*) variation on non-dimensional (X/D) distance. It has been observed from the figure that Nusselt number ratio from CFD is over predicting as compared to correlations data but trends are similar of both results. Table 3 represents percentage difference of CFD results with previous researcher's correlations data.

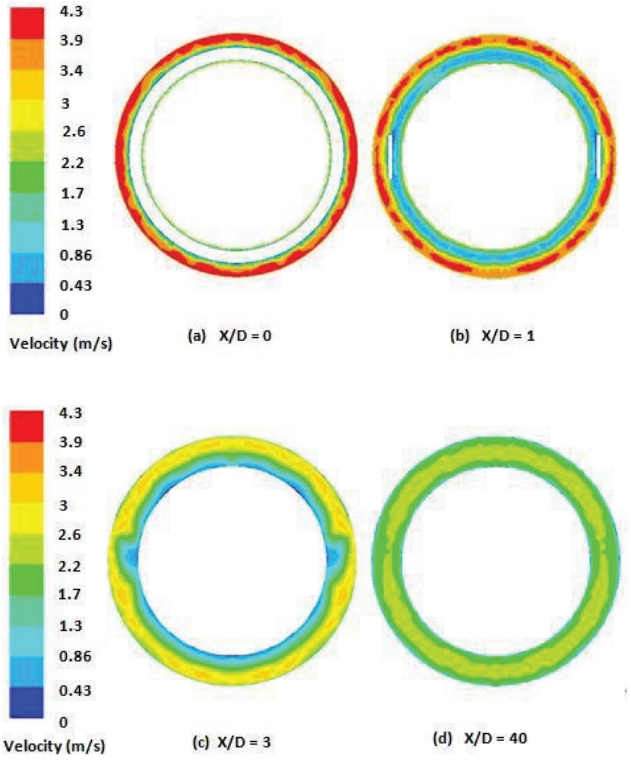

Figure 14. Velocity contours in axial flow direction (At X/D = 0, 1, 3 and 40).

The average values of percentage differences of the CFD-Spacer without mixing vane and CFD-Spacer with mixing vane results against correlations data are 15% and 16.5%, respectively.

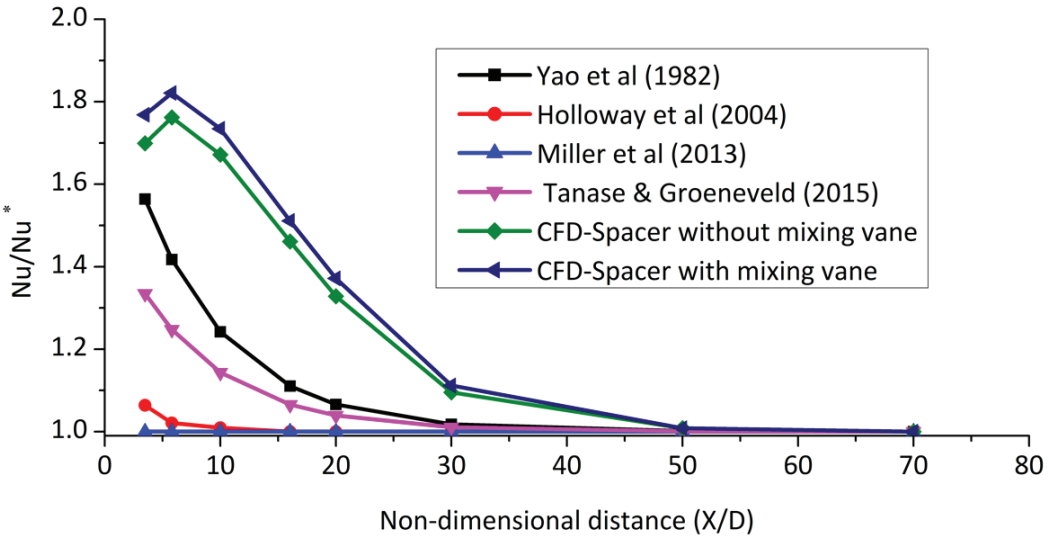

Figure 15. Comparison of correlations data with CFD results.

Table 3. Percentage difference of present CFD results with previous researcher's correlations data

Present Investigations	Percentage Difference with Previous Researcher's Correlations Data			
	Yao et al. (1982)	Holloway et al. (2004)	Millet et al. (2013)	Tanase & Groeneveld (2015)
CFD-Spacer without mixing vane	9.5 %	18 %	19 %	13.5 %
CFD-Spacer with mixing vane	11 %	19.5 %	20.5 %	15 %

CONCLUSION

This analysis represents the influences of spacer without mixing vane (i.e. spacer only) and spacer with mixing vane on the flow field & heat transfer characteristics of R134a (on supercritical pressure) within vertical flow annular channel. Simulations were conducted in ANSYS Fluent. The turbulent characteristic of flow has been modeled by using the turbulence model SST k-ω. The detailed comparative study for influences of spacer without mixing vane and spacer with mixing vane on flow field and heat transfer characteristics in downstream of the channel have been accomplished. Results are obtained for the spacer of blockage ratio 0.38, mass flow-rate 0.41469 kg/s, heat flux 160 kW/m^{2,} and 4.5 MPa system pressure. Results indicate that the reduction in surface temperature of the wall (which is around 2.5^{0}C) and the augmentation in the corresponding CHT is remarkable greater near downstream to spacer for the case of the spacer with mixing vane as compared to the spacer without mixing vane. Wall temperature fall and augmentation of CHT ensure the rods safety from greater surface temperatures. The spacer influence in improvement of the CHT/CHT* is observed up to the X/D = 40 in downstream, and then flow is found to be fully developed

Maximum axial velocity is observed at spacer point which is about 4.2 m/s. Due to the existence of mixing vane, velocity rises and fall in pressure are noted as higher at the zone, immediately behind the spacer downstream. The presence of mixing vane increases turbulent kinetic energy of the flow. The enhanced turbulent kinetic energy causes the improvement in heat transfer performance.

Nusselt number ratio from CFD is over predicting as compared to correlations data but trends are similar of both results. The average values of percentage differences of the CFD-Spacer without mixing vane and CFD-Spacer with mixing vane results against correlations data are 15% and 16.5%, respectively.

AUTHORSHIP CONTRIBUTIONS

Authors equally contributed to this work.

DATA AVAILABILITY STATEMENT

The authors confirm that the data that supports the findings of this study are available within the article. Raw data that support the finding of this study are available from the corresponding author, upon reasonable request.

CONFLICT OF INTEREST

The author declared no potential conflicts of interest with respect to the research, authorship, and/or publication of this article.

ETHICS

There are no ethical issues with the publication of this manuscript.

REFERENCES

[1] DOE US. Nuclear Energy Advisory Committee and Generation IV International Forum. A Technology Roadmap for Generation IV Nuclear Energy System; 2002. Available at: https://www.gen-4.org/gif/upload/docs/application/pdf/2013-09/geniv-roadmap2002.pdf. Accessed Nov 6, 2023.

[2] Wang H, Bi Q, Yang Z, Gang W, Hu R. Experimental and numerical study on the enhanced effect of spiral spacer to heat transfer of supercritical pressure water in vertical annular channels. Appl Therm Eng 2012;48:436-445. [CrossRef]

[3] Ishiwatari Y, Hongo I, Oka Y, Morooka S, Saito T, Ikejiri S. Numerical analysis of heat transfer enhancement by grid spacers in supercritical water. NURETH-13: 13. international topical meeting on nuclear reactor thermal hydraulics; Kanazawa, Ishikawa (Japan); Shimbashi, Minato, Tokyo; 2009.

[4] Gang W, Bi Q, Yang Z, Wang H, Zhu X, Hao H, et al. Experimental investigation of heat transfer for supercritical pressure water flowing in vertical annular channels. Nucl Eng Des 2011;241:4045-4054. [CrossRef]

[5] Zhu Y, Laurien E. Numerical investigation of supercritical water cooling channel flows around a single rod with a wrapped wire. Proceedings of ICAPP, San Diego, California, USA; 2010.

[6] Yamagata K, Nishikawa K, Hasegawa S, Fujii T, Yoshida S. Forced convective heat transfer to supercritical water flowing in tubes. Int J Heat Mass Transf 1972;15:2575-2593. [CrossRef]

[7] Swenson HS, Carver JR, Kakarala CR. Heat transfer to supercritical water in smooth-bore tubes. J Heat Transf 1965;87:477-484. [CrossRef]

[8] Zhu X, Morooka S, Oka Y. Numerical investigation of grid spacer effect on heat transfer of supercritical water flows in a tight rod bundle. Int J Therm Sci 2014;76:245-257. [CrossRef]

[9] Xiao Y, Pan J, Gu H. Numerical investigation of spacer effects on heat transfer of supercritical fluid flow in an annular channel. Int J Heat Mass Transf 2018;121:343-353. [CrossRef]

[10] Holloway MV, McClusky HL, Beasley DE, Conner ME. The effect of support grid features on local, single-phase heat transfer measurements in rod bundles. J Heat Transf 2004;126:43-53. [CrossRef]

[11] Bhattacharjee S, Ricciardi G, Viazzo S. Comparative study of the contribution of various PWR spacer grid components to hydrodynamic and wall pressure characteristics. Nucl Eng Des 2017; 317:22-43. [CrossRef]

[12] Miller DJ, Cheung FB, Bajorek SM. On the development of a grid-enhanced single-phase convective heat transfer correlation. Nucl Eng Des 2013;264:56-60. [CrossRef]

[13] Ikeda K. CFD application to advanced design for high efficiency spacer grid. Nucl Eng Des 2014;279:73-82. [CrossRef]

[14] Yao SC, Hochreiter LE, Leech WJ. Heat-transfer augmentation in rod bundles near grid spacers. J Heat Transf 1982;104:76-81. [CrossRef]

[15] Wang Y, Ferng YM, Sun LX. CFD assist in the design of spacer-grid with mixing-vane for a rod bundle. Appl Therm Eng 2019;149:565-577. [CrossRef]

[16] Tanase A, Groeneveld DC. An experimental investigation on the effects of flow obstacles on single phase heat transfer. Nucl Eng Des 2015;288:195-207. [CrossRef]

[17] Eter A, Groeneveld D, Tavoularis S. Convective heat transfer in supercritical flows of CO2 in tubes with and without flow obstacles. Nucl Eng Des 2017;313:162-176. [CrossRef]

[18] Qu W, Yao W, Xiong J, Cheng X. Experimental study of pressure loss in a 5 × 5-rod bundle with the mixing vane spacer grid. Front Energy Res 2021;9:675494. [CrossRef]

[19] Yang P, Zhang T, Hu L, Liu L, Liu Y. Numerical investigation of the effect of mixing vanes on subcooled boiling in a 3 × 3 rod bundle channel with spacer grid. Energy 2021;236:121454. [CrossRef]

[20] Huang H, Chen C, Liu L, Liu Y, Li L, Yu H, et al. Study on flow boiling characteristics in rectangle channel after the formation of blisters. Front Energy Res 2021;9:676586. [CrossRef]

[21] Wang Y, Wang M, Ju H, Zhao M, Zhang D, Tian W, et al. CFD simulation of flow and heat transfer characteristics in 5×5 fuel rod bundles with spacer grids of advanced PWR. Nucl Eng Technol 2020;52:1386-1395. [CrossRef]

[22] Ahmadpour V, Rezazadeh S, Mirzaei I, Mosaffa AH. Numerical investigation of horizontal magnetic field effect on the flow characteristics of gallium filled in a vertical annulus. J Therm Eng 2021;7:984-999. [CrossRef]

[23] Verma TN, Sinha SL. Experimental and numerical investigation of contaminant control in intensive care unit: A case study of Raipur, India. J Therm Eng 2020;6:736-750. [CrossRef]

[24] Xiong J, Qu W, Zhang T, Chai X, Liu X, Yang Y. Experimental investigation on split-mixing-vane forced mixing in pressurized water reactor fuel assembly. Ann Nucl Energy 2020;143:107450. [CrossRef]

[25] Zhang S, Gu H, Cheng X, Xiong Z. Experimental study on heat transfer of supercritical Freon flowing upward in a circular tube. Nucl Eng Des 2014;280:305-315. [CrossRef]

[26] Cheng H, Zhao J, Rowinski MK. Study on two wall temperature peaks of supercritical fluid mixed convective heat transfer in circular tubes. Int J Heat Mass Transf 2017;113:257-267. [CrossRef]

[27] ANSYS Inc. Ansys Fluent 12.0 User's Guide. 2009. Available at: https://www.afs.enea.it/project/neptunius/docs/fluent/html/ug/main_pre.htm. Accessed Nov 7 2023.

[28] Jaromin M, Anglart H. A numerical study of heat transfer to supercritical water flowing upward in vertical tubes under normal and deteriorated conditions. Nucl Eng Des 2013;264:61-70. [CrossRef]

[29] Palko D, Anglart H. Theoretical and numerical study of heat transfer deterioration in high performance light water reactor. Sci Technol Nucl Install 2008;2008:1-5. [CrossRef]

[30] Liu CC, Ferng YM, Shih CK. CFD evaluation of turbulence models for flow simulation of the fuel rod bundle with a spacer assembly. Appl Therm Eng 2012;40:389-396. [CrossRef]

[31] Podila K, Rao Y. CFD modeling of turbulent flows through 5×5 fuel rod bundles with spacer-grids. Ann Nucl Energy 2016;97:86-95. [CrossRef]

[32] Sohag FA, Mohanta L, Cheung FB. CFD analyses of mixed and forced convection in a heated vertical rod bundle. Appl Therm Eng 2017;117:85-93. [CrossRef]

[33] Cheng S, Chen H, Zhang X. CFD analysis of flow field in a 5×5 rod bundle with multi-grid. Ann Nucl Energy 2017;99:464-470. [CrossRef]